Characterization of AV-nodal Properties during Atrial Fibrillation using a Multilevel Modelling Approach

Mikael Wallman[1], Frida Sandberg[2]

[1] Department of Systems and Data Analysis, Fraunhofer-Chalmers Centre, Gothenburg, Sweden
[2] Department of Biomedical Engineering and Center for Integrative Electrocardiology (CIEL), Lund University, Lund, Sweden,

Abstract

Atrial fibrillation (AF) is a common and increasingly prevalent condition in the western society. During AF, the AV-node controls ventricular response to the rapid atrial impulses. However, current research indicates that the individual variability in AV-nodal function is large. Thus, characterization of the AV-node is an important step in determining the optimal form of treatment on an individual basis. Here we employ a multilevel modeling approach, comparing a previously presented statistical model with a novel detailed network model of the AV-nodal function during AF. We demonstrate that both models can be fitted to generate output that closely resembles clinical ECG data, and that estimated parameters in the less complex model corresponds to limited ranges of parameters in the more complex model.

1. Introduction

Atrial fibrillation (AF) is one of the most common cardiac arrhythmias encountered in clinical practice, occurring in 1-2% of the general population. Rate-control of AF is a commonly used treatment and several randomized clinical trials have shown that it may be as effective as rhythm-control medication [1]. The atrioventricular node (AVN) plays an important role during AF since it prevents the heart from racing by blocking atrial impulses.

Recent findings suggest that the AVN consists of two distinct pathways, referred to as the slow pathway (SP) and the fast pathway (FP), joining at a central node (CN) connected to the bundle of His [2]. It is believed that the FP has a faster conduction time and a longer refractory period than the SP, giving rise to the complex rate dependent properties observed in the AVN function [3]. These properties in turn influence the ventricular response during AF. In order to optimize rate control and improve clinical decisions there is therefore a need for quick and reliable characterization of the individual AVN.

Only a few previous models of the human AVN exist. Notably, Lian et al. have proposed a model treating the AVN as a lumped structure characterised by its overall refractoriness and conduction time, intended for simulation of RR series that exhibit similar properties to those observed during AF [4]. Inada et al. have proposed a biophysically detailed model of the human AVN action potential, based on a previous human atrial model with ion channel conductivities modified based on human mRNA levels [5]. We have previously proposed an AVN model accounting for different SP and FP electrophysiological properties, allowing estimation of model parameters from the ECG using a maximum likelihood (ML) approach [6, 7]. The model has been used to assess the effect of rate control drugs on AVN properties in AF patients; the estimated changes in AVN functional refractory period were found to be in agreement with invasive clinical data [8]. However, a drawback with the model is that several different AVN properties are lumped in a few parameters. In order to create a more realistic model of the AVN function, a better understanding of the interaction between different electrophysiological properties is crucial. The purpose of the present study is to explore the properties of the individual AVN using a multilevel modelling approach.

2. Methods

In this work we combine a previously presented statistical model [7], with a novel, more detailed network model based on developments of graph based simulation methods in [9–11]. In both models, we assume that atrial impulses arrive randomly to the AVN according to a Poisson process with mean arrival rate λ, proportional to the atrial fibrillatory rate (AFR) estimated from the atrial activity of the ECG.

2.1. Statisticl Model

The statistical model has been described in [6, 7]. Briefly, each atrial impulse arriving at the AVN is as-

sumed to result in a ventricular activation, unless blocked by a refractory AVN. The SP and FP are characterised by their respective absolute refractory period τ_s and τ_f corresponding to the shortest possible time between conducted impulses, and their relative refractory period $\tau_{p,s}$ and $\tau_{p,f}$ stochastically modelling prolongation of τ_s and τ_f due to e.g. concealed conduction. The proportion of atrial impulses conducted through the SP is quantified by the parameter α. Apart from AFR, the parameters, i.e. $\tau_s, \tau_f, \tau_{p,s}, \tau_{p,f}$ and α, are all estimated from the RR interval series by means of ML-estimation.

2.2. Network Model

The network model consists of 30 nodes connected in a Y-shape, with 10 nodes in each branch of the structure. Each node has two dynamical properties, refractory time and conduction delay, governed by the following pair of equations:

$$R_n = R_{min,r} + \Delta R_r(1 - e^{-DI_n/\tau_{R,r}}) \quad (1)$$

$$D_n = D_{min,r} + \Delta D_r e^{-DI_n/\tau_{D,r}} \quad (2)$$

Here, R stands for refractory time and D stands for delay, $n = 0...29$ is an index over nodes, and r is an index over branches (either FP, SP or CN). Further, R_{min} and D_{min} are the smallest possible refractory time and conduction delay respectively, and ΔR and ΔD are the maximal prolongations in refractory time and delay. DI is the diastolic interval, computed as the time from the end of the last refractory period until a new stimulation arrives at a given node. Finally, τ_R and τ_D are time constants. Thus, R_{min}, D_{min}, ΔR, ΔD, τ_R and τ_D constitute the model parameters. The general structure of the model is illustrated in Fig. 1.

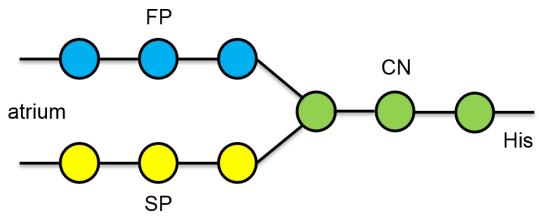

Figure 1. The figure shows the general structure of the detailed network model. Colors correspond to unique parameter sets for FP (blue), SP (yellow) and central node (green) respectively. For simplicity, only 3 out of 10 nodes for each branch are shown, but the full model comprises 30 nodes as stated above.

Parameters are shared between all nodes in each branch (marked FP, SP and CN in Fig. 1). Thus, with 3 parameters in each of Eqs. 1 and 2, the model has a total of 18 parameters. To simulate conduction through the model, we assume that the outermost nodes SP and FP are simultaneously activated by impulses generated by a Poisson process as described above. We then employ a modified Dijkstra's algorithm, as described in [10], to compute arrival times of the impulses in all nodes while dynamically updating the R and D properties. Finally, we derive RR-intervals by measuring the time lag between consecutive impulses reaching the outermost node of the CN branch. The network model is able to reproduce realistic RR-histograms (as shown in Sec. 3), as well as a number of experimentally and clinically observed features, such as rate dependent switching between branches, facilitation and concealed conduction.

2.3. ECG Analysis

RR-series and AFR obtained from 30 min segments of ECG from 3 patients were used to explore the relationship between the models. The ECG segments were extracted from 24-h Holter recordings at baseline in the RATAF (RATe control in Atrial Fibrillation) database [12]. AFR was determined from the f-waves, using spatiotemporal QRST cancellation [13], and subjected to spectral analysis using a HMM-based frequency tracking [14]. The mean impulse arrival rate λ was obtained by correcting AFR to take the atrial depolarization time into account [7]. Ectopic beats were detected based on heartbeat morphology, using a method described in [15]. RR intervals preceding and following ectopic beats were excluded from further analysis. This rendered one RR-series and one λ-value per patient.

2.4. Parameter Estimation from RR-series

In order to use the RR-series and λ-values (as described in 2.3) to estimate parameters for network model (described in 2.2), a genetic algorithm was employed. The algorithm used a population of 200 parameter sets in each generation, and a fitness function computed as the sum of squared differences between the bins of the histograms of measured and computed RR-series (bin centres between 250 ms and 1800 ms in steps of 50 ms), multiplied by -1. Here, minimal and maximal refractory times of the SP were required to be smaller than corresponding values for the FP, while minimal and maximal conduction delays of the SP were required to be larger than corresponding values for the FP.

Parameters for the 200 parameter sets were randomly initialized in the ranges $R_{min,r} = 250 - 580$ ms, $\Delta R_r = 0 - 600$ ms, $\tau_{R,r} = 50 - 250$ ms, $D_{min,r} = 0 - 20$ ms, $\Delta D_r = 0 - 50$ ms, and $\tau_{D,r} = 50 - 250$ ms. For each generation, 5000 impulses from a Poisson process were fed into SP and FP using each of the 200 parameter sets. This generated 200 fitness values, of which the 20 high-

est survived to the next generation. The 20 survivors were randomly divided into 100 potentially intersecting pairs, with each pair giving rise to a member of the next generation by contributing parameter values to the new individual with equal probability for each parameter. To maintain diversity, each parameter was given a 10% chance of mutation to a new random value. The algorithm was terminated when the highest fitness value crossed a threshold of -0.001. At that point, the fittest parameter set was stored and the algorithm reset. The described procedure was repeated 1000 times for each of the three RR-series, rendering 1000 parameter sets for each patient.

3. Results

Figure 2 shows RR-histograms for the three patients, derived as described in 2.4, together with corresponding histograms from the network model and fitted PDFs from the statistical model. Since 1000 different parameter sets per patient were estimated for the network model, only one representative histogram per patient is shown in the figure.

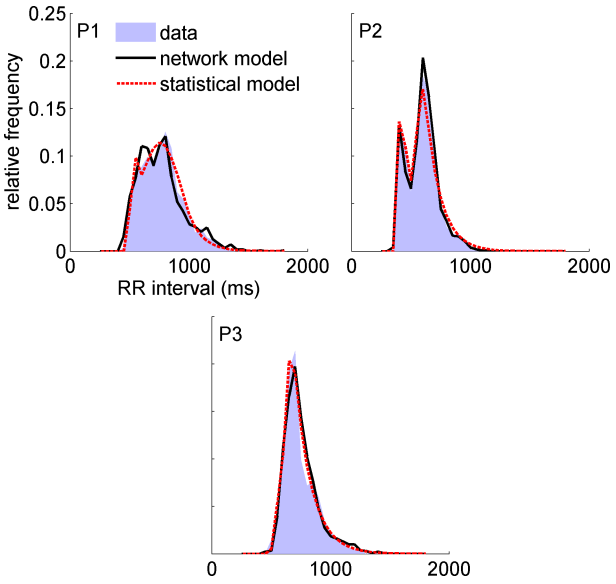

Figure 2. The figure shows RR-histograms derived from data (blue area), from the detailed network model (black solid line, representative examples), together with RR-interval PDFs from the statistical model (red dashed line) for the three patients (P1-P3 from left to right).

Inspecting the histograms in Fig. 2, some interesting dissimilarities can be noted with respect to modality: the histogram corresponding to P3 is tall and narrow, while that corresponding to P2 has two distinct peaks. In between the two is P1, with a small peak around 700 ms and a distinct one around 820 ms. As further shown in Fig. 2, the RR interval histograms generated using the network model and the fitted statistical model PDFs closely resemble the histograms obtained from the ECG signals. Close inspection of Fig. 2 reveal that the network model gives a slightly higher incidence of long RR-intervals compared to the ECG recordings, a phenomenon encountered for the majority of parameter sets (data not shown). Also, the simulated histogram for P1 has a higher and earlier first peak compared to the ECG data, which is seen in many of the parameter sets (data not shown), as well as in the corresponding PDF of the statistical model. For both models, possible causes for mismatches include the model structure itself, the modelling of the atrial impulses or the parameter fitting procedure.

Next, each of the 3000 parameter sets for the network model was used each parameter set to determine the effective and functional refractory periods (ERP and FRP). Here, ERP was taken to be equal to $R_{min,r}$, while FRP was computed from simulations as the shortest RR-interval resulting from two consecutive impulses through a given pathway. In the statistical model, FRPs of SP and FP were taken to be equal to τ_s and τ_f, respectively. Additionally, minimum and maximum conduction delay through the AVN for the network model were taken to be $D_{min,r}$, and $D_{min,r} + \Delta D_r$ respectively. Results are shown in Fig. 3.

Inspecting Fig. 3, it is obvious that the left column (showing ERPs and FRPs) contains the largest inter-individual differences. The general trend is for the SP properties to be more well constrained than the FP properties, likely owing to the fact that the SP will be the preferred conduction path for high frequency impulses due to its shorter refractory period. Further, we see that FRP is generally more constrained than the ERP. This is especially obvious for the SP of P2, with a 95% interval of 56 ms, spanning 333-389 ms. For all patients and both pathways, the 95% intervals of FRP derived from the network model contain the FRP estimate from the statistical model.

Considering the right column of Fig. 3, showing estimated conduction delays, we see that all three patients display similar ranges, and similar degrees of overlap between the 95% boxes for SP and FP, suggesting that the conduction parameters are harder from the data used here. However, at a significance level of $p < 0.05$, $D_{min,r}$ and ΔD_r for both SP and FP are correlated with one or several refractory time parameters, suggesting that some information about the conduction delays can be inferred from the data.

4. Conclusions

We demonstrate that a fixed set of statistical properties for the RR-series correspond to limited ranges of electrophysiological properties of the AVN, and that these can be estimated from ECG. The estimates suggest that the re-

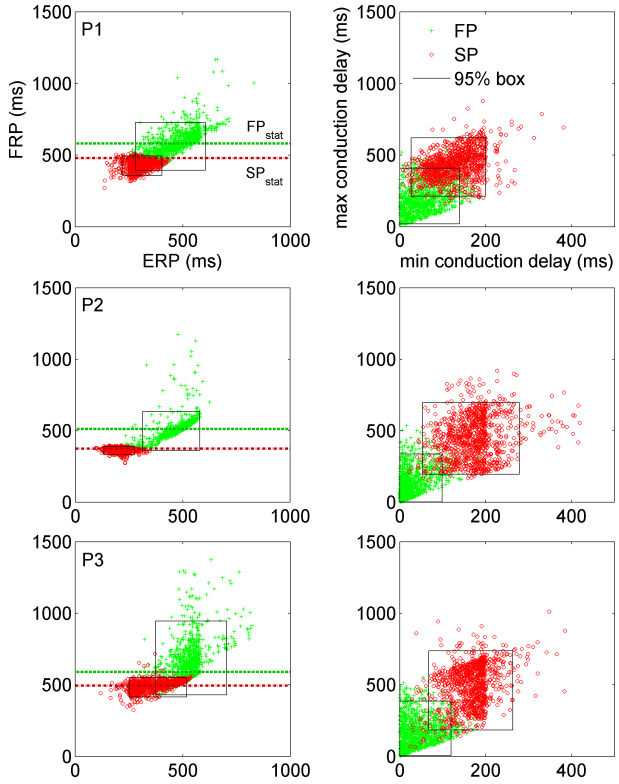

Figure 3. Each row (patients 1-3) shows 1000 sets of ERPs and FRPs (left column) and minimal and maximal conduction delays (right column) for SP (red o) and FP (green +). Black rectangles are the minimum-area boxes including 95% of the estimated parameters. Estimates of the FRP from the statistical model are shown as dashed and dashed-dotted lines in the left column.

fractory properties of FP and SP play a larger role than the conduction delay in the emergence of bimodal RR-series under AF.

5. Acknowledgements

The authors are grateful to Drs. Arnljot Tveit and Sara Ulimoen, Baerum Hospital, Drammen, Norway, for generously sharing the RATAF database. The authors acknowledge support from the Swedish Research Council, grant no. 621-2014-6134.

References

[1] European Heart Rhythm Association, European Association for Cardio-Thoracic Surgery, Camm A, Kirchhof P, Lip G, Schotten U, et al. Guidelines for the management of atrial fibrillation. European Heart Journal 2010;31:2369–2429.

[2] Kurian T, Ambrosi C, Hucker W, Fedorov VV, Efimov IR. Anatomy and electrophysiology of the human av node. Pacing Clin Electrophysiol 2010;33:754–762.

[3] Billette J, Tadros R. Integrated rate-dependent and dual pathway av nodal functions: principles and assessment framework. Am J Physiol Heart Circ Physiol 2014; 306:H173–83.

[4] Lian J, Müssig D, Lang V. Computer modeling of ventricular rhythm during atrial fibrillation and ventricular pacing. IEEE Trans Biomed Eng 2006;53:1512–1520.

[5] Inada S, Boyett M, Dobrzynski H. Mathematical models of human sinus and atrioventricular node action potentials. In Computers in Cardiology, 2009. 2009; 77–80.

[6] Corino VDA, Sandberg F, Mainardi L, Sörnmo L. An atrioventricular node model for analysis of the ventricular response during atrial fibrillation. IEEE Trans Biomed Eng 2011;58:3386–3395.

[7] Corino VDA, Sandberg F, Lombardi F, Mainardi L, Sörnmo L. Atrioventricular nodal function during atrial fibrillation: Model building and robust estimation. Biomed Signal Process Control 2013;8:1017–1025.

[8] Non-invasive assessment of the effect of beta blockers and calcium channel blockers on the AV node during permanent atrial fibrillation ;.

[9] Wallman M, Smith NP, Rodriguez B. A comparative study of graph-based, eikonal, and monodomain simulations for the estimation of cardiac activation times. IEEE Trans Biomed Eng 2012;59(6):1739–1748.

[10] Wallman M, Bueno-Orovio A, Rodriguez B. Computational probabilistic quantification of pro-arrhythmic risk from scar and left-to-right heterogeneity in the human ventricles. In Computing in Cardiology Conference (CinC), 2013. September 2013; 711–714.

[11] Wallman M, Smith NP, Rodriguez B. Computational methods to reduce uncertainty in the estimation of cardiac conduction properties from electroanatomical recordings. Med Image Anal ;18(1). ISSN 1361-8415.

[12] Ulimoen S, Enger S, Carlson J, Platonov P, Pripp A, Abdelnoor M, Arnesen H, Gjesdal K, Tveit A. Comparison of four single-drug regimens on ventricular rate and arrhythmia-related symptoms in patients with permanent atrial fibrillation. Am J Cardiol 2013;111(2):225–30.

[13] Stridh M, Sörnmo L. Spatiotemporal QRST cancellation techniques for analysis of atrial fibrillation. IEEE Trans Biomed Eng 2001;48(1):105–111.

[14] Sandberg F, Stridh M, Sörnmo L. Frequency tracking of atrial fibrillation using hidden Markov models. IEEE Trans Biomed Eng 2008;55:502–511.

[15] Lagerholm M, Peterson C, Braccini G, Edenbrandt L, Sornmo L. Clustering ECG complexes using Hermite functions and self-organizing maps. IEEE Trans Biomed Eng 2000;47(7):838–848. ISSN 0018-9294.

Address for correspondence:

Mikael Wallman
mikael.wallman@fcc.chalmers.se